Semiconductor and Metal Nanoparticle Formation on Polymer Spheres Coated with Weak Polyelectrolyte Multilayers

Peter Schuetz[†] and Frank Caruso*[,‡]

Max Planck Institute of Colloids and Interfaces, D-14424 Potsdam, Germany, and Centre for Nanoscience and Nanotechnology, Department of Chemical and Biomolecular Engineering, The University of Melbourne, Victoria 3010, Australia

Received January 6, 2004. Revised Manuscript Received May 25, 2004

We report the in situ formation of semiconductor and metal nanoparticles (NPs) on colloid particles precoated with weak polyelectrolyte multilayers. Poly(acrylic acid) (PAA)/poly(allylamine hydrochloride) (PAH) multilayers were assembled on the colloid spheres by the layer-by-layer technique and by exploiting copper ions as templating entities, as demonstrated by us earlier (*Adv. Funct. Mater.* **2003**, *13*, 929). Metal sulfide and metallic nanoparticles (NPs) were formed within PAH/PAA multilayers assembled on the polymer spheres by the adsorption of metal ions onto uncompensated functional groups of the polyelectrolytes (carboxylate or ammonium moieties), followed by reaction with hydrogen sulfide or sodium borohydride. Coating architectures comprising single or multi-shell NP layers were prepared, depending on the combination and sequence of weak and strong polyelectrolytes used for confining nanoparticle formation. The presence of the NPs within the polyelectrolyte matrixes was confirmed by UV−vis spectroscopy, energy-dispersive X-ray analysis, and transmission electron microscopy. We demonstrate that the method used permits the formation of organic−inorganic heterostructures incorporating a diverse range of NPs, ranging from sulfides such as PbS to metals such as gold.

Introduction

Nanoparticles (NPs) are important and versatile building blocks for the construction of functional nanoscale materials and devices,[2−5] such as two- and three-dimensional film assemblies[6−14] and designed colloidal aggregates,[15−18] as well as NP-based photovoltaic,[19,20] electroluminescence,[21−23] and sensing[24] devices. To enlarge and diversify the range of possible applications of these materials, the ability to create systems with vertical order is essential. One of the most adaptable techniques for the formation of thin films with highly defined structural order, as well as composition and thickness, is the electrostatic layer-by-layer (LbL) technique.[25−27] This method is based on the sequential deposition of oppositely charged species onto a substrate. Since its introduction in 1991 by Decher et al. for the assembly of thin polyelectrolyte multilayer films,[25] it has been expanded to include a wide range of different building blocks (e.g., nanoparticles, proteins, dyes) and substrates.[28] Frequently, and in particular

* To whom correspondence should be addressed. Tel: +61 3 8344 3461. Fax: +61 3 8344 4153. E-mail: fcaruso@unimelb.edu.au.
[†] Max Planck Institute of Colloids and Interfaces.
[‡] The University of Melbourne.

(1) Schuetz, P.; Caruso, F. *Adv. Funct. Mater.* **2003**, *13*, 929.
(2) Niemeyer, C. M. *Angew. Chem., Int. Ed.* **2001**, *40*, 4128.
(3) Shipway, A. N.; Katz, E.; Willner, I. *Chem. Phys. Chem.* **2000**, *1*, 18.
(4) *Clusters and Colloids. From Theory to Applications*; Schmid, G., Ed.; Wiley-VCH: Weinheim, 1994.
(5) *Nanoparticles and Nanostructured Films. Preparation, Characterization and Applications*; Fendler, J. H., Ed.; Wiley-VCH: Weinheim, 1998.
(6) Kiely, C. J.; Fink, J.; Brust, M.; Bethell, D.; Schiffrin, D. J. *Nature* **1998**, *396*, 444.
(7) Whetten, R. L.; Khoury, J. T.; Alvarez, M. M.; Murthy, S.; Vezmar, I.; Wang, Z. L.; Stephens, P. W.; Cleveland, C. L.; Luedtke, W. D.; Landman, U. *Adv. Mater.* **1996**, *8*, 428.
(8) Giersig, M.; Ung, T.; LizMarzan, L. M.; Mulvaney, P. *Adv. Mater.* **1997**, *9*, 570.
(9) Gittins, D. I.; Bethell, D.; Nichols, R. J.; Schiffrin, D. J. *Adv. Mater.* **1999**, *11*, 737.
(10) Schmitt, J.; Decher, G.; Dressick, W. J.; Brandow, S. L.; Geer, R. E.; Shashidhar, R.; Calvert, J. M. *Adv. Mater.* **1997**, *9*, 61.
(11) Feldheim, D. L.; Grabar, K. C.; Natan, M. J.; Mallouk, T. E. *J. Am. Chem. Soc.* **1996**, *118*, 7640.
(12) Cassagneau, T.; Fendler, J. H. *J. Phys. Chem. B* **1999**, *103*, 1789.
(13) Velev, O. D.; Tessier, P. M.; Lenhoff, A. M.; Kaler, E. W. *Nature* **1999**, *401*, 548.
(14) Jiang, P.; Cizeron, J.; Bertone, J. F.; Colvin, V. L. *J. Am. Chem. Soc.* **1999**, *121*, 7957.
(15) Alivisatos, A. P.; Johnsson, K. P.; Peng, X. G.; Wilson, T. E.; Loweth, C. J.; Bruchez, M. P.; Schultz, P. G. *Nature* **1996**, *382*, 609.
(16) Mirkin, C. A.; Letsinger, R. L.; Mucic, R. C.; Storhoff, J. J. *Nature* **1996**, *382*, 607.
(17) Shenton, W.; Davis, S. A.; Mann, S. *Adv. Mater.* **1999**, *11*, 449.
(18) Connolly, S.; Fitzmaurice, D. *Adv. Mater.* **1999**, *11*, 1202.
(19) Wang, Y.; Herron, N. *Chem. Phys. Lett.* **1992**, *200*, 71.
(20) Kotov, N. A.; Dekany, I.; Fendler, J. H. *J. Phys. Chem.* **1995**, *99*, 13065.
(21) Mattoussi, H.; Radzilowski, L.; Dabbousi, B. O.; Thomas, E. L.; Bawendi, M. G.; Rubner, M. F. *J. Appl. Phys.* **1998**, *83*, 7965.
(22) Colvin, V.; Schlamp, M. C.; Alivisatos, A. *Nature* **1994**, *370*, 345.
(23) Gao, M.; Richter, B.; Kirstein, S. *Adv. Mater.* **1997**, *9*, 802.
(24) Park, S. J.; Taton, T. A.; Mirkin, C. A. *Science* **2002**, *295*, 1503.
(25) Decher, G.; Hong, J. D. *Ber. Bunsen-Ges. Phys. Chem.* **1991**, *95*, 1430.
(26) Decher, G.; Hong, J. D.; Schmitt, J. *Thin Solid Films* **1992**, *210−211*, 831.
(27) Decher, G. *Science* **1997**, *277*, 1232.
(28) Bertrand, P.; Jonas, A.; Laschewski, A.; Legras, R. *Macromol. Rapid Comm.* **2000**, *21*, 319.

10.1021/cm049957h CCC: $27.50
Published on Web 07/15/2004

with NPs, uniform and dense surface coverages, with maximal particle densities, are desirable. For example, of special interest is the formation of dense layers of metal NPs with a uniform thickness (or continuous metal coatings) on colloid particles, as theoretical models predict unique and highly useful optical characteristics for such systems (i.e., strong absorbance in the IR-range, the potential to form complete optical band-gap materials, etc.).[29−31] However, studies that involve depositing *preformed* NPs from aqueous media have commonly only yielded surface coverages of up to ~0.3. The main reason for these relatively low surface coverages has been attributed to the strong electrostatic repulsion between the adsorbing NPs, thus limiting further adsorption after a certain coverage.[10,29,32−36] Recently, however, we reported that gold NPs stabilized with the weakly bound agent 4-(dimethylamino)pyridine yield dense and homogeneous NP coatings when deposited onto polyelectrolyte multilayer-coated particles.[37]

An alternative approach to the formation of NP-composite layers from preformed NPs is to synthesize the NPs in a preassembled matrix material. For example, the matrix can be a polymer that includes reactive sites that bind metal ions, which then can be converted to NPs following a reaction sequence. This approach was first applied to a system of a cast film of an ethylene and methacrylic acid copolymer. The acid groups of the film were loaded with lead ions, followed by a reaction with hydrogen sulfide (H_2S) gas yielding lead sulfide (PbS) NPs of adjustable size.[38] Later, the same procedure was also shown to work for, among others, photoluminescent, doped zinc sulfide (ZnS) NPs.[39,40] Possible models to describe the particle growth were reported.[41] A similar procedure was also applied to LB films of long chain carboxylic acids and amines. In that work, metal ions were complexed to the charged groups from a subphase or by immersion into a salt solution and then converted into the corresponding sulfides, selenides (e.g., PbS, CdS, ZnS, CdSe),[42−44] or metals (Pd, Pt).[45] As the acidic groups are regenerated during the conversion step, in some of the mentioned systems the possibility to repeat the reaction cycle of ion loading and conversion to NPs was demonstrated.[43] This reloading step generally leads to an increase in the size of the NPs.[39] A similar approach was used by Dai and Bruening to form metallic silver NPs by the reduction of silver ions complexed to poly(ethyleneimine), which was used for film assembly.[46] Recently, it was shown by Rubner and co-workers that the same principle can be also used to form NPs inside layers of weak polyelectrolytes (poly(acrylic acid), PAA, and poly(allylamine hydrochloride), PAH) containing uncompensated carboxylic acid groups.[47] These functional groups were obtained by assembling the films from solutions with pH values where the polyelectrolytes are only weakly charged.[48] Using this approach in combination with films comprising weak polyelectrolytes separated by interlayers of strong polyelectrolytes, vertically structured films of NP-rich and NP-free zones on *planar supports* were obtained.[47] In our earlier work we reported that the assembly of PAH/PAA films on colloid particles from PAA and PAH in their weakly charged state yielded only very thin layers and that colloidal stability of the particles was compromised, leading to particle aggregation.[49] This limits the formation of colloidally stable colloids with uniform layers of NPs in polyelectrolyte multilayers via the aforementioned approach.

In 2002, Bruening et al. reported a new method that provides uncompensated carboxylate groups inside polyelectrolyte (PAH/PAA) multilayers.[50] This method involves the complexation of a fraction of the carboxy-functions of the PAA chain with copper ions prior to film assembly. After formation, the films are exposed to acidic water, which reprotonates the acid groups and thus expels the copper ions, generating uncomplexed acid groups. We recently showed that this method could be used to form multilayers of PAH/PAA on colloid particles.[1] The multilayers were shown to grow regularly with an incremental thickness of around 1.5 nm per layer. As reported earlier for planar substrates,[50] the copper ions could be released, leaving uncompensated carboxylic groups.

In this paper, a combination of the two abovementioned techniques (i.e., "copper templating" of polyelectrolytes and in situ formation of NPs) is used to form NP-containing polymer thin films on colloid spheres. In the first part of the work, the previously described method[47] of adsorbing metal *cations* onto free carboxylic functions followed by conversion to NPs is employed. In the second part, we use a similar approach to demonstrate the formation of gold NPs using the *anionic* tetrachloroaurate ion ($AuCl_4^-$). Detailed studies were made to gain an understanding of the generation of such gold NPs. The obtained organic−inorganic composite films were studied by UV−vis spectroscopy, energy-

(29) Oldenburg, S. J.; Averitt, R. D.; Westcott, S. L.; Halas, N. J. *Chem. Phys. Lett.* **1998**, *288*, 243.
(30) Moroz, A. *Phys. Rev. Lett.* **1999**, *83*, 5274.
(31) Moroz, A. *Europhys. Lett.* **2000**, *50*, 466.
(32) Freeman, R. G.; Grabar, K. C.; Allison, K. J.; Bright, R. M.; Davis, J. A.; Guthrie, A. P.; Hommer, M. B.; Jackson, M. A.; Smith, P. C.; Walter, D. G.; Natan, M. J. *Science* **1995**, *267*, 1629.
(33) Musick, M. D.; Keating, C. D.; Keefe, M. H.; Natan, M. J. *Chem. Mater.* **1997**, *9*, 1499.
(34) Grabar, K. C.; Allison, K. J.; Baker, B. E.; Bright, R. M.; Brown, K. R.; Freeman, R. G.; Fox, A. P.; Keating, C. D.; Musick, M. D.; Natan, M. J. *Langmuir* **1996**, *12*, 2353.
(35) Ung, T.; Liz-Marzan, L. M.; Mulvaney, P. *J. Phys. Chem. B* **2001**, *105*, 3441.
(36) Dokoutchaev, A.; James, J. T.; Koene, S. C.; Pathak, S.; Prakash, G. K. S.; Thompson, M. E. *Chem. Mater.* **1999**, *11*, 2389.
(37) Gittins, D. I.; Susha, A. S.; Schoeler, B.; Caruso, F. *Adv. Mater.* **2002**, *14*, 508.
(38) Wang, Y.; Suna, A.; Mahler, W.; Kasowski, R. *J. Chem. Phys.* **1987**, *87*, 7315.
(39) Kane, R. S.; Cohen, R. E.; Silbey, R. *Chem. Mater.* **1996**, *8*, 1919.
(40) Kane, R. S.; Cohen, R. E.; Silbey, R. *Chem. Mater.* **1999**, *11*, 90.
(41) Kane, R. S.; Cohen, R. E.; Silbey, R. *Langmuir* **1999**, *15*, 39.
(42) Furlong, D. N.; Urquhart, R.; Grieser, F.; Tanaka, K.; Okahata, Y. *J. Chem. Soc., Faraday Trans.* **1993**, *89*, 2031.
(43) Urquhart, R. S.; Furlong, D. N.; Mansur, H.; Grieser, F.; Tanaka, K.; Okahata, Y. *Langmuir* **1994**, *10*, 899.
(44) Furlong, D. N.; Urquhart, R. S.; Grieser, F.; Matsuura, K.; Okahata, Y. *J. Chem. Soc. Chem. Commun.* **1995**, 1329.
(45) Elliot, D. J.; Furlong, D. N.; Gengenbach, T. R.; Grieser, F.; Urquhart, R. S.; Hoffman, C. L.; Rabolt, J. F. *Colloids Surf. A* **1995**, *103*, 207.
(46) Dai, J. H.; Bruening, M. L. *Nano Lett.* **2002**, *2*, 497.
(47) Joly, S.; Kane, R.; Radzilowski, L.; Wang, T.; Wu, A.; Cohen, R. E.; Thomas, E. L.; Rubner, M. F. *Langmuir* **2000**, *16*, 1354.
(48) Shiratori, S. S.; Rubner, M. F. *Macromolecules* **2000**, *33*, 4213.
(49) Kato, N.; Schuetz, P.; Fery, A.; Caruso, F. *Macromolecules* **2002**, *35*, 9780.
(50) Balachandra, A. M.; Dai, J. H.; Bruening, M. L. *Macromolecules* **2002**, *35*, 3171.

dispersive X-ray (EDX) analysis, and transmission electron microscopy (TEM). The main advantages of the in situ synthesis of NPs on colloid particles compared with the adsorption of *preformed* NPs are: (i) particle aggregation can be significantly reduced or eliminated, as nanoparticle formation can be confined within inner polyelectrolyte layers; and (ii) multi-shell NP structures can be formed by judicious selection of the polyelectrolyte multilayer composition and structure and by using several post-assembly steps involving inorganic reactants.

Experimental Section

Materials. Quartz substrates for UV−vis measurements were purchased from Hellma (Jena, Germany). Gold TEM grids were bought from Plano (Wetzlar, Germany). The PS spheres of diameter 496 nm were obtained from Microparticles (Berlin). Sodium sulfide (Na_2S), copper chloride ($CuCl_2$), lead acetate ($PbAc_4$), tetrachloroauric acid ($HAuCl_4$), silver nitrate ($AgNO_3$), and hydrochloric acid (HCl) were obtained from Sigma-Aldrich. The polyelectrolytes, poly(acrylic acid) sodium salt (PAA; M_W 5000), poly(allylamine hydrochloride) (PAA; M_W 70 000), poly(diallyldimethylammonium chloride) (PDDA; M_W 100 000), and poly(ethyleneimine) (PEI; M_W 25 000) were used as obtained from Sigma-Aldrich. Poly(styrenesulfonate) (PSS; M_W 70 000) was purchased from Sigma-Aldrich and dialyzed prior to use. The water for all experiments was prepared in a Milli-Q system and had a resistivity higher than 18.2 MΩ cm.

Substrate Preparation. Quartz slides (for UV−vis experiments) were first cleaned by ultrasonication in 2-propanol for 5 min. They were then hydrophilized by immersion in a solution containing 100 mL of NH_4OH (29 wt % aqueous solution), 100 mL of H_2O_2 (30 wt % aqueous solution), and 500 mL of water at 70 °C for 10 min, followed by rinsing with copious amounts of water (***Caution:*** Mixtures of ammonium hydroxide and hydrogen peroxide are extremely corrosive).

Multilayer Assembly on Planar Substrates. The multilayers were assembled by the electrostatic LbL technique as described previously.[1] For adsorption the polyelectrolytes PAA and PAH were prepared as 40 mM solutions with respect to the monomeric units, containing 3.5 mM copper chloride and 0.5 M sodium chloride, which were adjusted to a pH value of 5.5. All substrates were first primed with a layer of PEI by exposing them to a 1 mg mL^{-1} solution for 20 min and rinsing several times with water. The layers of the weak polyelectrolytes PAA and PAH were then assembled by consecutively dipping the PEI-coated substrates into the respective polyelectrolyte solutions for at least 20 min, and rinsing thoroughly with deionized water. To obtain similar systems as used for the colloidal substrates (see below), three layers of strong polyelectrolytes (i.e. PSS/PDDA/PSS) were adsorbed as final layers. The PSS and PDDA solutions contained 1 mg mL^{-1} polyelectrolyte and 0.5 M NaCl. For measurement, the substrates were dried in a nitrogen flow.

Multilayer Assembly on Colloids. Multilayers of the weak polyelectrolytes PAA and PAH were adsorbed on 640-nm diameter PS spheres using the electrostatic LbL method, as described previously.[1] The polyelectrolytes were alternately deposited from the respective solutions (containing 40 mM (monomeric units) polyelectrolyte, 3.5 mM $CuCl_2$, and 0.5 mM NaCl at a pH of 5.5) for 20 min, followed by four cleaning cycles of centrifugation and redispersion in water. After adsorption of PAH, the dispersions were washed with water containing 3.5 mM $CuCl_2$ to prevent the leaching of copper ions from the layers. Following adsorption of four PAH/PAA bilayers, several layers of strong polyelectrolytes in the sequence PSS/PDDA/PSS were deposited onto the particles to maintain the colloidal stability of the particles during the varied reaction conditions. PSS and PDDA were adsorbed from solutions containing the polyelectrolytes at a concentration of 1 mg mL^{-1} and 0.5 M NaCl.

Formation of NPs. After the formation of the polyelectrolyte multilayers, the templating copper ions were removed by diluting the dispersions with diluted HCl of pH 3.3. (Slides were immersed in diluted HCl of pH 3.3.) The metal ions (e.g., Pb^{2+}, Ag^+) were incorporated into the layers by treating the films with 1 mM solutions of the soluble metal salts (e.g., $PbAc_4$, $AgNO_3$) at a neutral pH. The metal ions were transformed to the respective sulfides by bubbling freshly generated H_2S gas through the colloidal dispersion or the immersion solution of the slides (formed by the reaction of HCl and Na_2S; ***Caution***: toxic gas, use closed vessels and work under a fume hood). The reaction was allowed to proceed for 2 h, after which the substrates were thoroughly washed as described before.

For the formation of gold NPs, the copper ions were removed as described before. The substrates were then treated with a $AuCl_4^-$ solution at a pH of 3. The gold ions were finally reduced with an ∼10 mM aqueous solution of $NaBH_4$. After reaction and a ripening time of 1 h, the samples were washed as described above.

Transmission Electron Microscopy (TEM). Approximately 3 μL of the diluted particle suspensions was dried on carbon-coated copper grids. TEM images were then taken with a Zeiss EM 912 Omega microscope at an acceleration voltage of 120 kV.

Energy Dispersive X-ray (EDX) Experiments. EDX spectra were recorded with a Phillips CM 12 electron microscope equipped with an EDX attachment.

UV−Vis Measurements. UV−vis spectra of films prepared on quartz substrates were recorded on a HP 8453 spectrophotometer.

Results and Discussion

Polyelectrolyte Multilayer Formation. A method similar to the one described by Bruening and coworkers[50] was applied to deposit PAH/PAA multilayers onto both planar (quartz and gold) substrates and PS spheres. This method exploits the presence of small concentrations (mM range) of copper ions to complex a fraction of the carboxylate groups of PAA. We recently reported the layer growth behavior and properties of PAH/PAA films assembled via this approach.[1] It was found that the multilayers grow regularly on PS or silica microspheres (diameter ∼400−500 nm), yielding an incremental thickness of about 3 nm per PAH/PAA bilayer, as determined by the optical technique of single particle light scattering. Further, the ζ-potentials of the coated particles were adjusted to achieve maximum colloidal stability by using a solution of copper chloride for the washing steps after the deposition of PAH. These deposition conditions allowed the deposition of at least 5 PAH/PAA bilayers without noticeable aggregation of the coated particles. UV−vis spectroscopy and EDX measurements confirmed the incorporation of Cu^{2+} ions into the PAH/PAA films in the form of complexes with the carboxylate functions of PAA. It was also shown that the complexed Cu^{2+} could be subsequently released from the films by treatment with hydrochloric acid at pH 3 for 60 min. This procedure protonates the carboxylate groups of PAA and thus destroys the complex with the Cu^{2+}, releasing Cu^{2+}. After washing with water at neutral pH, uncomplexed PAA carboxylate groups are available in the film. This is confirmed by the disappearance of the copper-carboxylate band at 260 nm,[51] as can be seen by UV−vis spectroscopy on quartz slides (Figure 1a, spectra 1 and 2). To avoid having lowly

(51) Koide, M.; Tsuchida, E.; Kurimura, Y. *Macromol. Chem. Phys.* **1981**, *182*, 359.

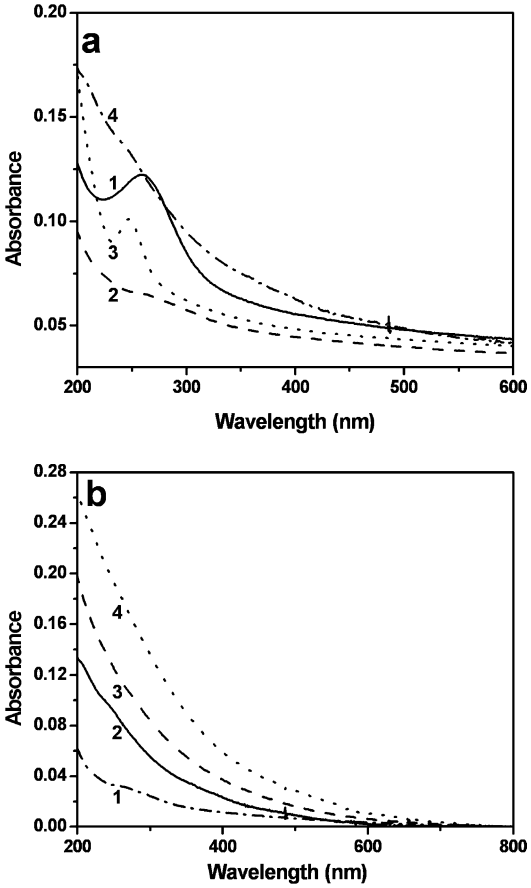

Figure 1. UV-vis spectra of PbS NPs in PAH/PAA multilayers deposited onto quartz substrates. The final film structure is PEI/$(PAH/PAA)_4$/PAH/PSS/PDDA/PSS. (a) Steps involved in the formation of the PbS NPs: multilayer film with complexed Cu^{2+} (1); removal of Cu^{2+} (2); adsorption of Pb^{2+} (3); reaction with H_2S to form PbS NPs (4). (b) Multiple adsorption/reaction cycles. Film (as in part a) without NPs (1) and after one (2), two (3) and three (4) adsorption/reaction cycles.

charged particles during the acid treatment step, which can induce particle aggregation, three layers of the strong polyelectrolytes PSS and PDDA (i.e., PSS/PDDA/PSS) were assembled on top of the PAH/PAA multilayers. This was the case for all systems (colloid- and planar substrate-supported films) in all of the following experiments, unless otherwise mentioned. The final film structure was $(PAH/PAA)_4$/PAH/PSS/PDDA/PSS.

PbS Nanoparticle Formation. The films, which at pH > 5 contain carboxylate moieties, can be loaded with a variety of metal ions. These metal ions in turn may be transformed into sulfide or metal NPs.[47] To this end, the PAH/PAA multilayer films were immersed in a 1 mM solution of different metal salts ($PbAc_4$ and $AgNO_3$) following the removal of the copper ions and neutralization. The formation of NPs inside the polyelectrolyte multilayer films was first studied by UV−vis spectroscopy on planar (quartz) substrates. Figure 1a shows the UV−vis spectra for the different steps of the formation of PbS NPs. During the adsorption of Pb^{2+} in the PAH/PAA layers, a new absorption peak at 245 nm emerges (spectrum 3). After exposure of the multilayer films to gaseous H_2S, an absorption spectrum representative of semiconducting NP dispersions is seen (spectrum 4). As the PbS NPs are not monodisperse in size, it is difficult to discern the peak for the energy of the excitons, but a very weak shoulder can be found in some spectra at around 230 nm (corresponding to about 5 eV). As the precise location of this shoulder cannot be determined, the exact size cannot be directly deduced from these data using the published tables; however, a rough estimate leads to a particle diameter from 1 to 1.5 nm.[52] An approximate determination of particle size is also possible from the position of the absorption edge in the visible range of the spectrum.[38,52] As this edge is not well defined in our spectra, taking the upper limit value of ca. 600 nm would indicate that the PbS NPs are smaller than ∼2.5 nm. The existence of these sub-4-nm particles is consistent with the UV−visible data and the findings of Rubner et al.,[47] who reported the formation of particles with a diameter of 2 nm in a similar system.

Because during the reaction of Pb^{2+} with H_2S the carboxylate sites of PAA are transformed back to their uncomplexed state, repetition of the described loading and reaction cycle is possible, which may increase the amount of PbS NPs in the layers. The UV−vis spectra resulting from such experiments (Figure 1b) show an increased absorbance after each cycle in the region below 600 nm, which is characteristic for PbS NPs. Because these spectra show no clear exciton peaks and because a possible shift in the position of the absorption edge toward higher wavelengths is not conclusive, it is not possible to discern whether the higher content of PbS in the layers is due to the formation of more NPs or the growth of existing NPs. To address this issue and to obtain more information on the surface density of the NPs, experiments were conducted on PAH/PAA films assembled on TEM grids, which were used as substrates. The carbon films on TEM grids were coated under the same conditions as for the quartz slides. The use of gold grids was necessary, as copper grids corroded during the polyelectrolyte deposition steps. After the deposition and removal of Cu^{2+}, the films were loaded with Pb^{2+} and exposed to H_2S gas. The TEM images of these samples (Figure 2) show a homogeneous film, but no individual particles are discernible after one reaction cycle. After a second reaction cycle, the grain size of the coating increased and some larger nanoparticles with a size of about 4−5 nm can be discerned.[53]

A similar approach was used to form silver NPs inside PAH/PAA multilayers. Silver ions were infiltrated into the layers from a 1 mM $AgNO_3$ solution. The reduction of these ions with dissolved $NaBH_4$ formed silver NPs, which showed a clearly discernible plasmon peak at 422 nm (see Supporting Information). However, these NPs were not stable toward oxidation as the plasmon peak vanished after exposure of the films to air or water for 4 h. Although this plasmon peak reappeared upon an additional reduction step with $NaBH_4$, due to the air and water sensitivity of this system these experiments were not extended to particle systems.

Following the experiments on the quartz substrates, PAH/PAA-coated PS spheres of diameter ∼500 nm were used as supports for the formation of semiconductor nanoparticles. After the removal of complexed Cu^{2+} by HCl, the coated PS spheres were dispersed in a solution of $PbAc_2$ (1 mM) to load them with Pb^{2+}. These ions were

(52) Henglein, A. *Chem. Rev.* **1989**, *89*, 1861.
(53) An exact evaluation of the sizes was not possible as the weak contrast of PbS did not allow the use of higher magnifications.

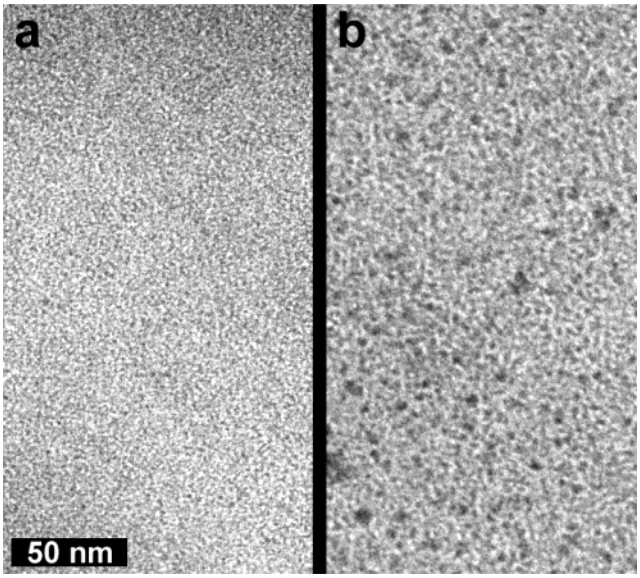

Figure 2. TEM images of PbS NPs formed in PEI/(PAH/PAA)$_4$/PAH/PSS/PDDA/PSS films deposited on gold TEM grids. The images correspond to PbS nanoparticles prepared with one (a) or two (b) adsorption/reaction cycles, obtained by using the same TEM magnification.

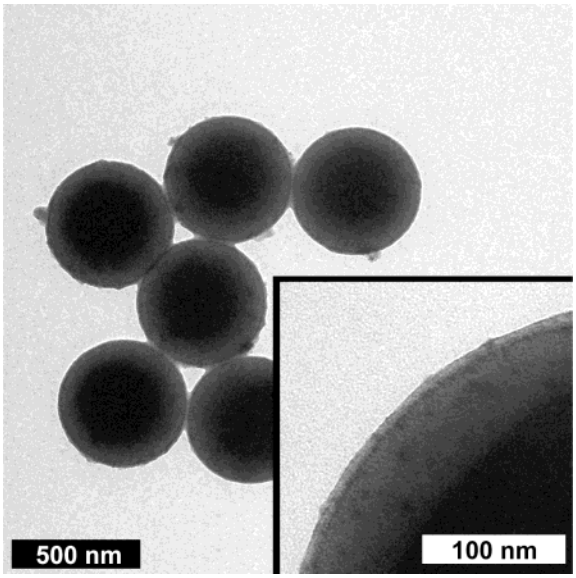

Figure 3. TEM images for PbS NPs formed in (PAH/PAA)$_4$/PAH/PSS/PDDA/PSS films on the surface of 496-nm-diameter PS spheres. The inset shows a magnification of the particle surface where the NPs can be seen as high-contrast dots.

then turned into PbS NPs by bubbling hydrogen sulfide (ca. 4−5 mL) through the particle dispersion (1 mL), followed by shaking the sealed reaction vessel for 12 h to maximize the uptake and reaction of H_2S in the liquid phase. The colloids were then washed three times by centrifugation and redispersion in water. After this procedure, a brown centrifugation pellet of the coated particles indicated the formation of PbS NPs. TEM imaging revealed the presence of PbS NPs on the particles (Figure 3). Because of the weak contrast and the curved nature of the films it is difficult to determine the size of the nanoparticles and the extent of surface coverage. However, similar nanoparticle sizes and coverage to that observed on the planar substrates (TEM grids) is most plausible. EDX experiments further confirmed the presence of lead on the particle surface (data not shown). Importantly, there were no signs of aggregation of the NP-coated spheres. Overall, the above data show that polyelectrolyte films of PAH and PAA deposited onto PS spheres can be exploited to synthesize semiconductor NPs, yielding NP-functionalized beads that are colloidally stable.

Gold Nanoparticle Formation. While decreasing the pH of the solution (pH ∼3) in which PAH/PAA polyelectrolyte multilayers are immersed, it is possible to protonate the amine groups of PAH (pK_a (PAH) ∼8.5)[49,54] to give quaternary ammonium groups. These can then act as positively charged sites for adsorption of anionic precursors. We explored this possibility to form gold NPs inside PAH/PAA multilayers assembled on quartz substrates. Following the removal of the originally bound Cu^{2+}, the multilayers were treated with a diluted solution of tetrachloroauric acid ($HAuCl_4$, 0.025%$_{wt}$) at a pH of 3. After washing four times with water to remove any excess ions, a solution of freshly dissolved $NaBH_4$ in water (0.5 mg mL^{-1}) was added. The mixture was allowed to react for 60 min, and the films were then thoroughly washed with water. UV−vis spectra of the quartz-supported PAH/PAA films indicate the incorporation of gold species, as absorption at ∼230 nm (here a shoulder to the PSS absorption peak at ∼227 nm) and broadening of the spectrum are observed (Figure 4a, spectrum 2). After reduction with $NaBH_4$, this shoulder disappears and the typical shape of spectra representative of nanometer-sized particles emerges, with a gradual decline in absorbance from 250 to ca. 650 nm (Figure 4a, spectrum 3). Only in some of the recorded spectra a very weak shoulder can be seen in the range of ca. 520 nm, indicating that the majority of the particles are of size below ca. 4−5 nm, where no plasmon absorbance occurs. Repetition of the loading and reduction cycle leads to a stronger gold NP plasmon peak at ca. 530 nm for two cycles, which is then red-shifted to 550 nm after three cycles (Figure 4b). This plasmon peak is predominantly due to the formation of larger gold NPs and/or aggregates of smaller NPs. This is confirmed by TEM (see later).

To prove that the formation of the gold NPs is restricted to within the layers of weak polyelectrolytes, a series of control experiments on substrates coated with other polyelectrolyte combinations was performed (data not shown). Multilayers of PSS/PDDA, PSS/PAH, PAA/PDDA, and PAA/PAH on quartz slides were treated as described above. UV−vis spectra of the films on quartz slides were measured to monitor the uptake of $AuCl_4^-$ and the formation of the gold NPs. The intensity of the absorbance for the $AuCl_4^-$ uptake corresponds directly to the intensity found for the absorbance band of the gold particles. The PAA/PAH multilayers gave the highest intensities, followed by the PAA/PDDA and PSS/PAH films, which showed 70% and 30%, respectively, of the magnitude of the value observed for the PAA/PAH films. No $AuCl_4^-$ incorporation and no nanoparticle formation were evident in the layers assembled from the two strong polyelectrolytes PSS/PDDA. This indicates that the adsorption of $AuCl_4^-$ is a cumulative effect of the PAH and PAA groups in the films. As men-

(54) Burke, S. E.; Barrett, C. J. *Langmuir* **2003**, *19*, 3297.

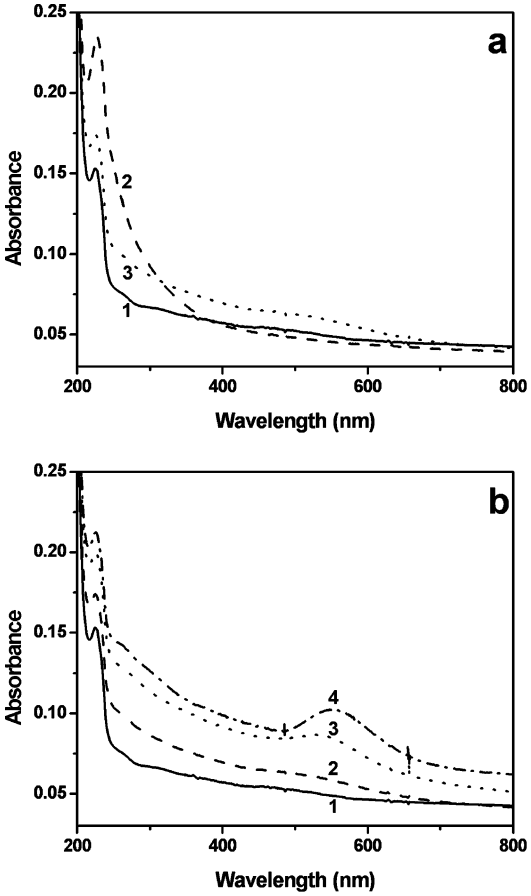

Figure 4. UV-vis spectra for the formation of gold NPs in PAH/PAA multilayers assembled on quartz substrates. The final film structure is PEI/$(PAH/PAA)_4$/PAH/PSS/PDDA/PSS. (a) Spectra shown are for the films before (1) and after (2) loading with $AuCl_4^-$ ions, and after reaction with $NaBH_4$ to form the gold NPs (3). (b) The film as in part (a) before (1) and after one (2), two (3), and three (4) adsorption/reaction cycles.

tioned earlier, it is likely that by lowering the pH of the solution to which the multilayers are exposed previously, uncharged amine groups (of PAH) become protonated to ammonium groups. It is also plausible that at the same time carboxylate groups (of PAA) become protonated, which in turn may free previously complexed PAH ammonium groups to interact with new incoming anions such as $AuCl_4^-$. A further enhancement of the adsorption of anions may originate from the formation of hydrogen bonds between the protons of the carboxylic acid groups and the chloride atoms of $AuCl_4^-$. This reasoning most probably explains the confinement of the formation of gold NPs to the PAA/PAH layers, in contrast to the PSS/PDDA layers. Experiments involving colloid particles provide further proof for this (see later).

As the UV spectra allow neither the determination of the particle density nor an estimate of the predominant size of the particles (as the intensity of the plasmon peak increases dramatically for sizes above ca. 4−5 nm diameter), experiments on TEM grids were made to visualize the NPs. TEM analysis shows that the particles form a homogeneous layer with the majority of the particles ~3−4 nm in size (Figure 5a). Some larger particles can be seen as well, accounting for the plasmon peak observed in UV−vis spectroscopy.

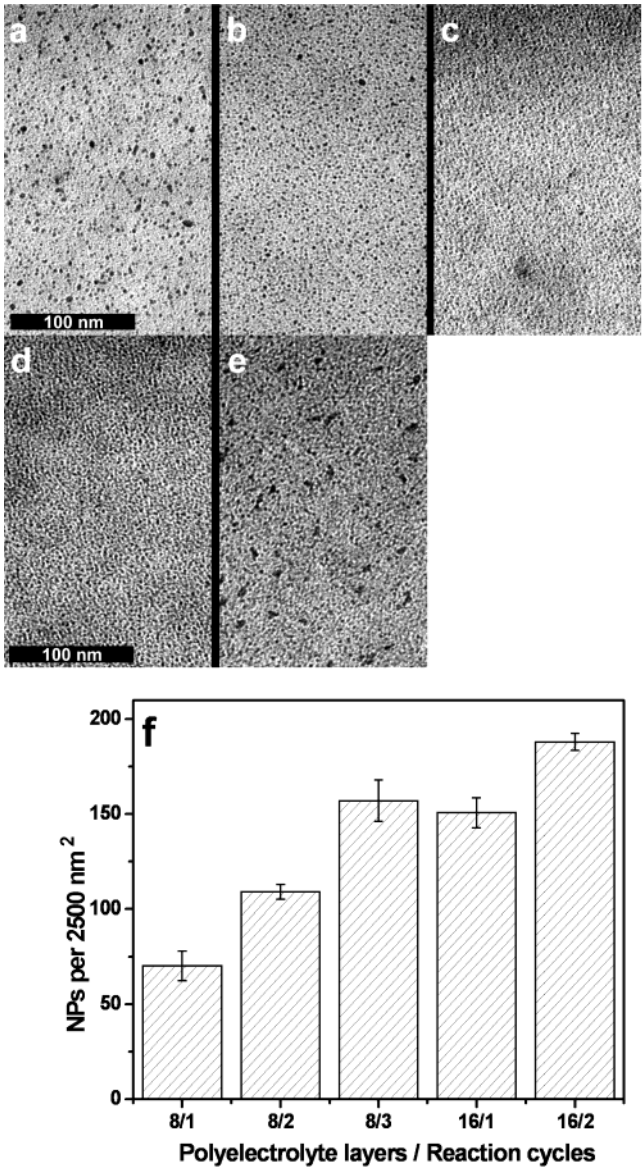

Figure 5. TEM images of gold NPs formed in films of PEI/$(PAH/PAA)_x$/PAH/PSS/PDDA/PSS ($x = 4$ or 8) on gold grids. Images (a)−(c) correspond to one, two, and three adsorption/reaction cycles for a film with 8 layers of weak polyelectrolytes ($x = 4$), and images (d) and (e) correspond to one and two adsorption/reaction cycles for a film comprising 16 layers of weak polyelectrolytes ($x = 8$). For all TEM images the same magnification was used. Part (f) shows the results of the numerical evaluation of the images (a)−(e). Two images from two independent samples were taken for each condition. The particles were manually counted in an area of 50 nm × 50 nm. The average results including error bars are shown. Columns 1−5 correspond to the images (a)−(e), respectively.

By repeating the loading and reduction cycle an increase in the particle density was observed, as shown in Figures 5a−c for one, two, and three cycles, respectively. A numerical evaluation of the particle numbers in an area of 50 nm × 50 nm is shown in Figure 5f (first three columns). An increase of the particle number from ca. 70 ± 8 (one cycle) to 109 ± 4 (two cycles) and 157 ± 11 (three cycles) in the selected areas was obtained, while the particle size remained virtually constant. This corresponds to an increase in particle number of about 50% per cycle. These data clearly show that in the case

of gold NPs, repeated cycles lead to predominantly an increase in number, but not in size, of the NPs.

Another possibility to enhance the area density of the NPs is the deposition of thicker films of the weak polyelectrolytes. To investigate this effect, films comprising sixteen (instead of eight) layers of the weak polyelectrolytes were assembled on the TEM grids. The final film structure, including the primer and outermost layers was PEI/$(PAH/PAA)_8$/PAH/PSS/PDDA/PSS. After reduction of the adsorbed gold species the films showed a density of 151 ± 8 NPs per 250 nm^2 (Figure 5d), which is double the value found for corresponding films with only eight layers of PAA/PAH. Following a second adsorption and reduction cycle, a further increase to around 188 ± 4 NPs was observed (Figure 5e). It is noted that at these higher NP densities, many of the NPs overlap making the particle counting less and less accurate. The size of most of the NPs, however, remains around 4 nm, although some larger NPs are also seen. By assuming an average diameter for the NPs, these data can be used to calculate the surface coverage as a ratio between the area of the NPs and the imaged area. By assuming a diameter of 3 nm (which is a lower estimate), the coverage obtained with this method is similar to (ca. 20%, Figure 5a) or higher than (ca. 50%, Figure 5e) previously published data for NPs deposited from aqueous solutions, which show coverages up to ca. 30%.[10,29,32−36] These experiments show that the size of the NPs is reproducibly around 3−4 nm, that the individual particles mostly do not grow during further adsorption and recycle steps, and that the area density of the particles is proportional to the number of adsorption sites within the PAA/PAH film and that it increases with the number of reaction cycles.

As the gold NPs showed promising characteristics on planar supports, the system was applied to PS spheres to produce gold NP-coated spheres. A dispersion of the polyelectrolyte-coated PS particles was treated according to the procedure described for the planar supports. A first indication of the successful formation of gold NPs was the red color of the centrifugation pellet following the reduction of the gold ions. TEM images of the particles show that the reaction occurred mainly inside the layers, as even after only one washing step there were no free gold NPs found on the grids (Figure 6). Higher TEM magnification images of the particle surface show the gold NPs as small dark spots on the surface of the spheres (Figure 6 inset). From the TEM images, it is estimated that the diameters of the NPs are 3−4 nm, as on planar supports. EDX experiments confirmed the presence of gold on the microparticles (not shown).

We conducted further experiments to prove that the formation of the gold NPs only takes place in the layers of the weak polyelectrolytes and not in the layers of strong polyelectrolytes. Therefore, a different number of layers of the strong polyelectrolytes PSS and PDDA were adsorbed on top of the weak polyelectrolyte layers. In addition to the three layers already used to stabilize the particle charge, a further two and four PSS/PDDA layers were adsorbed. Figure 7a−c shows TEM images of the resulting particles. At the perimeter of the particles there is a "layer" of low contrast, and closer to the particle surface is another "layer" which has a high

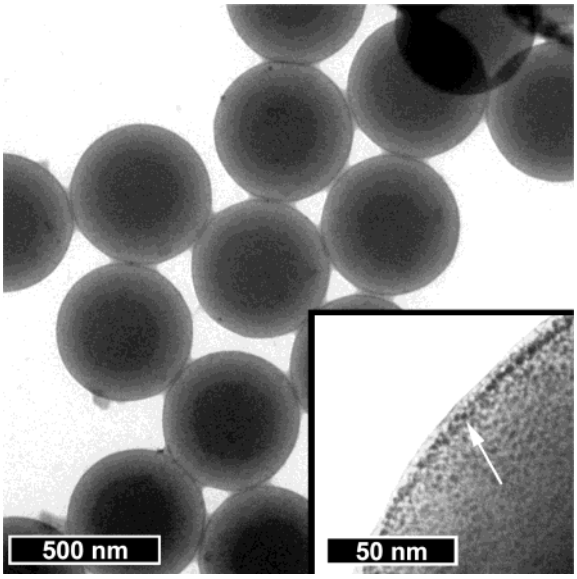

Figure 6. TEM images of gold NPs formed within PAH/PAA multilayer films deposited on 496-nm-diameter PS spheres. The final film structure is $(PAH/PAA)_4$/PAH/PSS/PDDA/PSS. The inset shows a higher magnification of the particle surface where the NPs can be seen as dark dots, as indicated by the arrow.

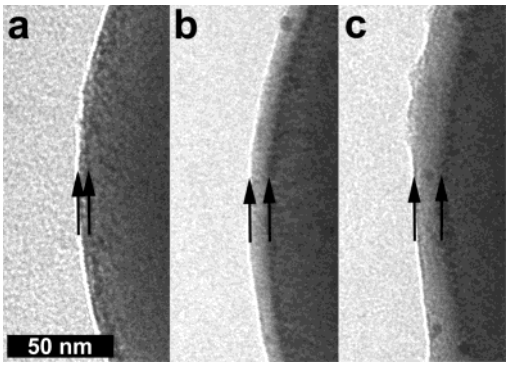

Figure 7. TEM images of the surface of 496-nm-diameter PS spheres coated with different polyelectrolyte layer structures and reacted to form gold NPs. On top of the weak polyelectrolyte film [$(PAH/PAA)_4$/PAH], three (a), five (b), and seven (c) layers of strong polyelectrolytes [$(PSS/PDDA)_{x=1,2,3}$/PSS] were adsorbed. The arrows indicate the thickness of the area with weak contrast, where virtually no gold NPs were formed.

contrast due to the gold NPs incorporated in the PAH/PAA layers (as indicated by the arrows). It can be seen that the thickness of the "layer" of low contrast is proportional to the number of the adsorbed layers of strong polyelectrolytes.

An interesting result that additionally confirms the confinement of the NPs within the layers of weak polyelectrolytes is the formation of structures with a double corona of gold NPs. A structure containing two ranges of weak polyelectrolyte layers separated by strong polyelectrolytes was assembled. The sequence of layers assembled was PEI/$(PAA/PAH)_4$/$(PSS/PDDA)_4$/PSS/PAH/$(PAA/PAH)_4$/PSS/PDDA/PSS. Following the formation of the gold NPs (as described above), two separate regions of gold NPs could be discerned, as indicated by the arrows in Figure 8. This provides a new means to prepare multi-shell NP coatings on spheres, which can display unique properties.[55] These systems

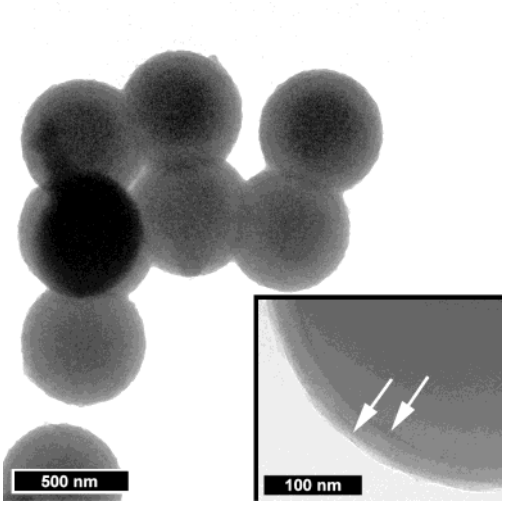

Figure 8. TEM images of PS particles coated with (PAH/PAA)$_4$/PAH/(PSS/PDDA)$_4$/PSS/(PAH/PAA)$_4$/PAH/PSS/PDDA/PSS. Two regions of weak polyelectrolytes are separated by strong polyelectrolytes. After the in situ formation of gold NPs, two distinct black rings can be seen (indicated by the arrows), representing two separate shells of gold NPs.

may also form the basis for the formation of continuous multiple metal shells on particles through electroless plating, where existing NPs are used as seeds for the growth of continuous and/or thicker gold layers. To this end, a 1:1-mixture of $HAuCl_4$ (1%$_{wt}$) and hydroxylamine (NH_2OH; 0.4 mM) was added stepwise to the NP-coated PS spheres and agitated. Good coating results were obtained upon addition of 25 μL (three times) of the plating solution to a dispersion of particles with a concentration of about 0.02 wt % (see Supporting Information). Growth and coalescence of the gold nanoparticles was observed as well as an increased surface roughness. The homogeneity of the coating depends on several parameters, including reactant concentrations, reaction time, and gold NP seed concentration in the polyelectrolyte films. We are currently investigating these issues to form metal-shell dielectric-core spheres through a variety of methods.

Conclusions

We have demonstrated that colloid particles coated with weak polyelectrolytes can be used for the confined synthesis of semiconductor and metal NPs through polyelectrolyte ion adsorption and subsequent conversion of these ions into NPs, yielding NP-coated dielectric spheres. The NPs formed are in the size range of mostly sub-2.5 nm for PbS and between 3 and 4 nm for gold. By repeating the adsorption/reaction cycles the NP loading incorporated in the multilayers increased systematically with the number of cycles performed. In the case of the gold NPs, the increased loading amounts are largely due to an increase in the number of particles. Particles with multiple and separated NP shells can also be prepared by confining the NP synthesis within layers of the weak polyelectrolytes PAH/PAA separated by stacks of strong polyelectrolytes. The method used allows the generation of core−shell particles with compositional and structural complexity, and they are likely to be of interest in a range of applications.

Acknowledgment. C. Pilz is thanked for general technical assistance and U. Blöck, Hahn-Meitner-Institute, Berlin, Germany, is thanked for the EDX measurements. H. Möhwald is acknowledged for support within the MPI Interface department. This work was funded by the BMBF within the framework of the Biofuture program, the Australian Research Council within the Federation Fellowship and Discovery Project schemes, and the Victorian State Government, Department of Innovation, Industry and Regional Development, Science, Technology and Innovation initiative.

Supporting Information Available: UV−vis spectra for the formation of Ag NPs in PAH/PAA multilayers deposited onto quartz substrates and TEM images of electroless plated gold NP-seeded coatings on 496-nm-diameter PS spheres (pdf). This material is available free of charge via the Internet at http://pubs.acs.org.

CM049957H

(55) Prodan, E.; Radloff, C.; Halas, N. J.; Nordlander, P. *Science* **2003**, *302*, 419.